Journal of Nonlinear Optical Physics & Materials
Vol. 25, No. 4 (2016) 1650045 (11 pages)

DOI: 10.1142/S0218863516500454

World Scientific
www.worldscientific.com

Shelf solutions and dispersive shocks in a discrete NLS equation: Effects of nonlocality

Panayotis Panayotaros

Departamento de Matemáticas y Mecánica,
Instituto de Investigaciones en Matemáticas Aplicadas y en Sistemas,
Universidad Nacional Autónoma de México,
Apdo. Postal 20–126, 01000 Cd. México, México
panos@mym.iimas.unam.mx

Received 12 September 2016

We study shelf-like breathers and dispersive shock phenomena in a discrete nonlinear Schrödinger (DNLS) equation with a nonlocal nonlinearity. The system models laser light propagation in waveguide arrays made from a nematic liquid crystal substratum. Shelf-like breathers are studied in the regime of small linear intersite coupling, and we report some new theoretical existence and stability results. We also study numerically the evolution from nearby dam-break and more general jump initial conditions for stronger linear intersite coupling. In the defocusing case, we see rarefaction and shock wave profiles, superposed with oscillations. Some of the hyperbolic features of the observed profiles are described approximately by continuous NLS hydrodynamics. Nonlocality is seen to lead to some smoothing of the rapid oscillations seen in the local DNLS.

Keywords: Discrete NLS; nonlinear lattices; nematic liquid crystals; breathers; dispersive shocks.

1. Introduction

The discrete nonlinear Schrödinger (DNLS) equation is a well-studied model of light propagation in structures with periodicity or more general spatial inhomogeneity in the directions perpendicular to the optical axis.[1,2] Such geometries have also been explored in highly nonlinear and nonlocal media such as nematic liquid crystals,[3–5] where the nonlocality leads to a DNLS equation with the Hartree-type cubic nonlinearity proposed by Fratalocchi and Assanto.[6] Related experimental work is also reported in Refs. 7–9. The present paper explores further some of the properties of this nonlocal DNLS, and the sometimes surprising differences with the standard cubic DNLS with power nonlinearity.

The special properties of the nonlocal model of Fratalocchi–Assanto[6] can be made more precise when we examine breather solutions, see Ref. 10 for some other properties. Nonlocality leads to well-localized breathers, but the linearization around these solutions has internal modes with appreciable amplitude in the

region of small breather amplitude.[11] The nonlocal system of Ref. 6 also has localized solutions with maximum amplitude at the interface between bright and dark regions.[11] In Sec. 2, we report some recent results on related "shelf-type" breather solutions for the nonlocal DNLS and its local limit, the standard cubic DNLS, see Ref. 12 for more mathematical details. As in other contexts, shelves (or "kinks") are solutions that asymptote to a nonzero value at $-\infty$, and decay at $+\infty$. We see that for small linear intersite coupling shelf-type breathers exist, and we also obtain results on their linearly stability.

Part of the motivation for studying shelf-type breathers is that they are near the dam-break initial conditions studied in continuous NLS equations[13] and more recently in nonlocal analogues.[14] Here, we are also interested in discrete analogues of more general jump initial conditions. In the continuous case, jump initial conditions lead to the formation of dispersive shock structures. The literature on these phenomena is extensive, see Ref. 14 for a list of references. In Sec. 3, we examine discrete analogues for both the nonlocal DNLS and its local limit. Note that small amplitude jumps for the power DNLS that have been studied in detail in Ref. 15.

In the defocusing case, a special feature of the DNLS equation is that, for small linear intersite coupling, the amplitude in the darker region does not increase significantly. For instance, the amplitude remains small in the dark region of the dam-break initial condition, in both the local and nonlocal systems. As the linear intersite coupling is increased, we start to see some of the continuous NLS hydrodynamic behavior for the amplitude and phase variables, such a rarefaction wave trailing a shock wave that moves into the small amplitude region at constant speed. We see that continuous NLS calculations, see e.g., Ref. 14, predict the rough geometry of the discrete shock reasonably well. Features such as the slope of the rarefaction wave, and the speed of the leading jump are not affected significantly by nonlocality. The main nonlocal effect is a smoothing of some of the features of the amplitude profile. For example, high frequency oscillations behind the leading jump seen for small nonlocality start to resemble smooth soliton wavetrains as we increase the nonlocality parameter.

Focusing DNLS equations with discrete jump initial conditions also exhibit interesting dynamics. We see a combination of large amplitude oscillations in the bright region with a slow transfer of energy to the darker region. This basic effect seems to be present in both the local and nonlocal systems. The present study of dispersive wave phenomena in DNLS is preliminary, and the explanation of many of our numerical results in Sec. 3 requires further work, see Sec. 4 for further comments.

2. Shelf Solutions in Discrete NLS Equations and Their Stability

The one-dimensional discrete NLS equation proposed in the study of nematic waveguide arrays[6] is

$$\dot{u}_n = \delta i(u_{n+1} + u_{n-1} - 2u_n) + 2\gamma \tanh \frac{\kappa}{2} i \left(\sum_{m\in\mathbb{Z}} e^{-\kappa|m-n|} |u_m|^2 \right) u_n, \quad n \in \mathbb{Z} \qquad (2.1)$$

with δ, γ, κ real constants, $\kappa > 0$. κ is the "nonlocality" parameter. We can also write (2.1) as a Hamiltonian system with Hamiltonian H given by

$$H = \delta \sum_{n\in\mathbb{Z}} |u_{n+1} - u_n|^2 - \gamma \tanh \frac{\kappa}{2} \sum_{n\in\mathbb{Z}} \sum_{m\in\mathbb{Z}} |u_m|^2 e^{-\kappa|m-n|} |u_n|^2, \tag{2.2}$$

see e.g., Ref. 11. An additional conserved quantity for suitably decaying solutions is the power $P = \sum_{n\in\mathbb{Z}} |u_n|^2$.

In the "local limit" $\kappa \to \infty$, we recover the well-known cubic discrete NLS. In the "nonlocal limit" $\kappa \to 0$ with P finite, e.g., suitably decaying initial conditions, (2.1) reduces to a linear system.

The effect of nonlocality in (2.1) can be seen quite precisely when we examine "breather" solutions and their linear stability. *Breathers* are solutions of (2.1) of the form $u_n = e^{-i\omega t} A_n$, with ω real, and $A : \mathbb{Z} \to \mathbb{C}$. By (2.1), A, ω then satisfy

$$-\omega A_n = \delta(A_{n+1} + A_{n-1} - 2A_n) + 2\gamma \tanh \frac{\kappa}{2} \left(\sum_{m\,\in\,\mathbb{Z}} e^{-\kappa|m-n|} |A_m|^2 \right) A_n, \quad \forall\, n \in \mathbb{Z}. \tag{2.3}$$

Equation (2.3) can be solved for A that decays as $n \to \pm\infty$, see Refs. 11, 16 and 17 for results of this type. We can also consider solutions that do not decay at infinity. In particular, a *shelf-type* breather is a solution of (2.3) satisfying $A_n \to A \neq 0$ as $n \to -\infty$, and $A_n \to 0$ as $n \to +\infty$.

Shelf-type breathers are first sought for $\delta = 0$, and then continued to $|\delta|$ small. For $\kappa > 0$, $\omega\gamma < 0$, these $\delta = 0$ solutions have the profile $A_n = \widetilde{A}_n$ with

$$\widetilde{A}_n = \begin{cases} \alpha & \text{if} \quad n < n_0, \\ \frac{\alpha}{\sqrt{1-\rho}} & \text{if} \quad n = n_0, \\ 0 & \text{if} \quad n > n_0 \end{cases} \tag{2.4}$$

with $\rho = e^{-\kappa}$, $\alpha^2 = \omega(-2\gamma \tanh(\frac{\kappa}{2}))^{-1} \frac{1-\rho}{1+\rho}$, see Ref. 12. The interface is at an arbitrary site n_0, and we also have more general solutions of (2.3) satisfying $|A_n| = \widetilde{A}_n$, for all integer n.

The main effect of the nonlocality is that the amplitude has its maximum at the interface n_0. In the local limit $\kappa \to \infty$, the amplitude at n_0 becomes α, and we recover the shelf breather solution of the power cubic DNLS. In Ref. 12, we prove that the solution (2.4) persists for $|\delta|$ sufficiently small, with a slightly perturbed profile. In particular, the amplitude has its maximum at n_0, and the same limiting values at $\pm\infty$.

It appears that solutions of (2.3) with different limiting amplitudes at $\pm\infty$ can not be obtained using the breather Ansatz and are in general two-periodic solutions, consider e.g., the case $\kappa \to \infty$, $\delta = 0$. The existence of such solutions for more general parameter values seems to be open.

To analyze the linear stability of solutions of (2.1), we use the variable v defined by $u = e^{-i\omega t} v$. The amplitude A of a breather solution is then a fixed point of the

evolution equation for v, and linear stability analysis is the study of the linearization around solutions $v = A$. To see the general structure of these equations, let $z = [q, p]^T$, where q, p are real functions on $\mathbb{Z}$ with $z_n = [q_n, p_n]^T$, $q_n = \mathrm{Re} v_n$, $p_n = \mathrm{Im} v_n$, $n \in \mathbb{Z}$. The linearization at a fixed point A is then

$$\dot{z} = J\mathcal{H}z, \tag{2.5}$$

with

$$J = \begin{bmatrix} 0 & I \\ -I & 0 \end{bmatrix}, \quad \mathcal{H} = \begin{bmatrix} L_+ & 0 \\ 0 & L_- \end{bmatrix}, \tag{2.6}$$

where

$$L_- = -\omega I - \delta\Delta + 2\mathcal{A}, \quad L_+ = -\omega I - \delta\Delta + 2\mathcal{A} + 4\mathcal{M}, \tag{2.7}$$

and $\mathcal{A}$, $\mathcal{M}$ are linear operators on real functions on $\mathbb{Z}$ defined by

$$\mathcal{A}(n,k) = \tanh\frac{\kappa}{2}\left(\sum_{m\in\mathbf{Z}} e^{-\kappa|m-n|}A_m^2\right)\delta_{n,k}, \quad n, \kappa \in \mathbb{Z}, \tag{2.8}$$

$$\mathcal{M}(n,k) = \tanh\frac{\kappa}{2}e^{-\kappa|n-k|}A_kA_n, \quad n, \quad k \in \mathbb{Z} \tag{2.9}$$

with $\delta_{n,k}$ the Kronecker delta.

The linear stability equations above can be used for both decaying and nondecaying breather solutions.[12]

The study of the spectrum of the operator $J\mathcal{H}$ around the small $|\delta|$ shelf solutions above is motivated by the question of the evolution from the vicinity of the shelf, and of possible quantitative changes as $|\delta|$ is increased, see Sec. 3.

The spectrum of $J\mathcal{H}$ for shelf-type breathers of both the local and nonlocal DNLS equations is studied in mathematical detail in Ref. 12, and we here outline the main results of that work. We remark that the theoretical analysis of the nonlocal case is not as complete, and only concerns the continuous spectrum of $J\mathcal{H}$ (numerical studies suggest the existence of point spectrum as well). Specifically, in Ref. 12, we fix $\gamma = -1$ (to simplify the notation) and show that for any given $\kappa > 0$ and $|\delta|$ sufficiently small, the essential spectrum of $J\mathcal{H}$ for the nonlocal shelf includes the set of $\lambda \in \mathbb{C}$ that satisfy $\lambda^2 \in B_1 \cup B_{2,\kappa}$, where B_1, $B_{2,\kappa}$ are the sets

$$B_1 = \left\{ -\left(\omega - 4\delta\sin^2\frac{k}{2}\right)^2 : \quad k \in \mathbb{R}) \right\}, \tag{2.10}$$

$$B_{2,\kappa} = \left\{ -4\delta\sin^2\frac{k}{2}\left(2\omega\frac{1-\rho^2}{1-2\rho\cos k+\rho^2} + 4\delta\sin^2\frac{k}{2}\right) : \quad k \in \mathbb{R}) \right\}, \tag{2.11}$$

where $\rho = e^{-\kappa}$. Clearly $\lambda^2 \in B_1$ implies λ imaginary. In the cases $\delta < 0$ (focusing), $\delta > 0$ (defocusing) $\lambda^2 \in B_{2,\kappa}$ implies λ real, imaginary, respectively.

In the defocusing case (2.10), (2.11) can be interpreted as describing two dispersion relations corresponding, respectively, to the linearization around the trivial

solution $A_n = 0$, for n (case $\lambda^2 \in B_1$), and around the constant solution $A_n = \alpha$, for all n, (case $\lambda^2 \in B_{2,\kappa}$). The result for the local limit is obtained by taking $\kappa \to \infty$ in (2.11). A technical detail is that in the local problem, the set of λ satisfying $\lambda^2 \in B_1 \cup B_{2,\infty}$ was shown to describe the essential spectrum completely. In the nonlocal problem, we have not ruled out a bigger set.

Note that in Ref. 11, we showed the existence of breathers that are continuations of $\delta = 0$ solutions of (2.3) with compact support consisting of a finite set of m consecutive sites. These solutions may be termed "finite shelf" breathers. For $\kappa > 0$, $\delta = 0$, and $m \geq 3$, their amplitude has its maximum at the two interface sites, and is constant at the $m - 2$ interior sites.[11] As $\kappa \to \infty$, we recover a solution of the power DNLS, with constant amplitude at the m sites as $\delta \to 0$. As we increase m by adding more sites to the left of the initial block, we have a breather that can be used as a decaying approximation of the (infinite) shelf of (2.4). Moreover, the band of the $\lambda^2 \in B_{2,\kappa}$ frequencies of the shelf appears to be the limit of point eigenvalues of the linearization around the finite shelf breathers. In the nonlocal DNLS, there is also evidence of eigenvalues that are outside this band, which leads us to think that the shelf spectrum may also contain point eigenvalues, see Fig. 3 of Ref. 11.

3. Discrete Riemann Problem for Local and Nonlocal DNLS

To study the evolution from a discrete analogue of the Riemann problem, we consider initial conditions

$$u_n(0) = \begin{cases} u_1 & \text{if} \quad n \leq n_0, \\ u_2 & \text{if} \quad n > n_0. \end{cases} \tag{3.1}$$

The case $u_2 = 0$ is the "dam-break problem", and we can consider $u_1 = \alpha$, i.e., an initial conditions that is close to a shelf-type breather.

In the numerical simulations, we use $N = 523$ sites with $n_0 = 261$. We also consider Dirichlet boundary conditions. Boundary effects at $N = 1{,}523$ seem negligible for the local DNLS, but somewhat more difficult to control in the nonlocal problem, unless the amplitude near the boundary is small. The results for the nonlocal problem therefore are more credible away from the boundary. Nevertheless, our observations on the nonlocal problem below seem to be independent of the apparent boundary effects. We note that the evaluation of the convolution in the nonlinearity is expensive and large domain integrations are significantly slower.

In what follows, we show results of the integration of the defocusing DNLS, starting with the local (cubic power) DNLS. As in the previous section, we fix $\gamma = -1$ so that defocusing corresponds to $\delta > 0$.

For small linear coupling δ, the amplitude profile is essentially that of the initial condition. This is indicated in Fig. 1, where $\delta = 0.05$ and we show the evolution from a dam-break initial condition. By (2.10), (2.11), with $\kappa \to \infty$, the nearby breather solution is linearly stable. A more general step initial condition, such as $u_1 = 1.0$, $u_2 = 0.5$, leads to similar behavior.

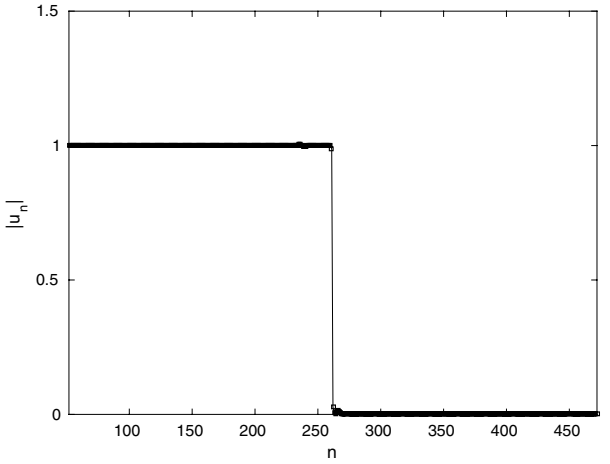

Fig. 1. Amplitude $|u_n|$ versus n at time $t = 60$, integration of cubic power DNLS. Initial condition $u_n = 1$ for $n \leq 261$, $u_n = 0$ for $n > 261$. $N = 523$, $\delta = 0.05$, $\gamma = -1.0$.

Increasing δ, we start to see a behavior that is closer to that of the continuous NLS. In Fig. 2, we show the evolution from dam-break initial condition $u_1 = 1.0$, $u_2 = 0$ with $\delta = -0.5$. In Fig. 3, we show the evolution from the step initial condition $u_1 = 1.0$, $u_2 = 0.5$, with $\delta = -0.5$. Larger δ leads to similar profiles. The figures suggest possible rarefaction waves and shock-like structures, superimposed with oscillations. Figure 3 suggests a shock joining the $|u_2| = 0.5$ amplitude value to an amplitude between 0.5 and 1. Behind this jump, we see an oscillatory region with an average level that is then joined to the $|u_1| = 1$ amplitude on the left by what looks like a rarefaction wave.

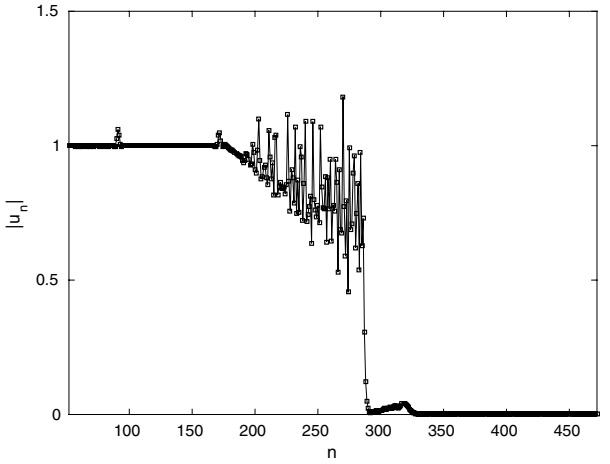

Fig. 2. Amplitude $|u_n|$ versus n at time $t = 60$, integration of cubic power DNLS. Initial condition $u_n = 1$ for $n \leq 261$, $u_n = 0$ for $n > 261$. $N = 523$, $\delta = 0.5$, $\gamma = -1.0$.

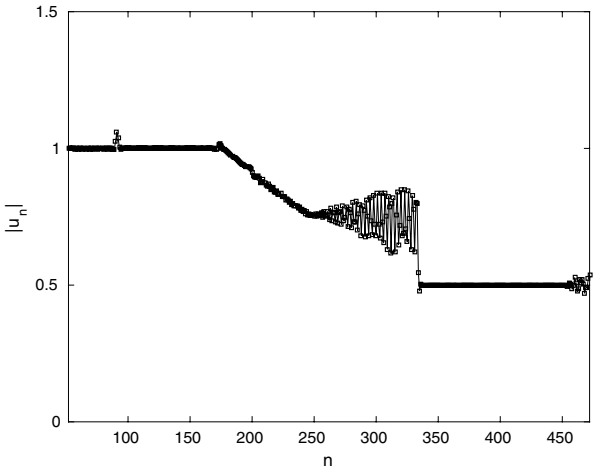

Fig. 3. Amplitude $|u_n|$ versus n at time $t = 60$, integration of cubic power DNLS. Initial condition $u_n = 1$ for $n \leq 261$, $u_n = 0.5$ for $n > 261$. $N = 523$, $\delta = 0.5$, $\gamma = -1.0$.

We have made a heuristic comparison of one of these profiles to solutions of the well-known system of conservation laws obtained from the continuous cubic NLS in hydrodynamic form. Specifically, we consider the cubic NLS

$$u_t = \delta i u_{xx} + 2i\gamma|u|^2 u \tag{3.2}$$

with $\gamma = -1$, i.e., compare to (2.1), and use the variables r, v, where $u = \sqrt{r}e^{i\theta}$, and $v = \partial_x\theta$. We then examine the well-known hyperbolic system for $r > 0$, v (obtained from the evolution equations for r, v, with terms proportional to r_{xx}, r_x^2 omitted).

The choice of parameters $\gamma = -1$, $\delta = 0.5$ in (3.2) are those used recently in Ref. 14, and we can readily compare Fig. 3 with the solution (5.1)–(5.5) of Ref. 14 (setting $q = 1$), describing precisely a shock leading a rarefaction wave connecting an intermediate amplitude value to the leftmost amplitude u_2.

We examine three features of the numerical profiles of Fig. 3:

(i) The hyperbolic system for r, v predicts a slope $-(3\sqrt{2}t)^{-1}$ for the rarefaction wave.[14] Figure 3 for $t = 60$ suggests that the rarefaction fan has a width of ~ 75 points, and connects the values $|u| = 1$ on the left to $|u| = 0.75$ at $n \sim 245$. The value $|u| = 0.75$ is an average of the oscillatory region behind the leading jump. The numerical slope is then -0.0033, while the hyperbolic theoretical slope at $t = 60$ is -0.0039.

(ii) The leftmost and rightmost points $x_L(t)$, $x_R(t)$ of the rarefaction fan of the hyperbolic system are

$$x_L(t) = -\sqrt{2r_I}t + x_0, \quad x_R(t) = -(2\sqrt{2r_I} - 3\sqrt{2r_D})t + x_0, \tag{3.3}$$

where r_I, r_D are the values of $|u|$ at the left and right of the wave, and x_0 is the initial position of the discontinuity.[14] Here $r_I = 1$, $x_0 = 261$, and we

use the numerical value $r_D = 0.75$, which is the (average) value of $|u|$ at the apparent end of the fan: in Fig. 3 this is at $n \sim 245$. At $t = 60$, (3.3) yields $x_L(60) = 176$, $x_R(60) = 209$, while Fig. 3 suggest $x_{L,\mathrm{num}}(60) = 175$, $x_{R,\mathrm{num}}(60) = 245$. The discrepancy at the leading amplitude may be due to some finer structure between the apparent leftmost and rightmost points of the fan, $n = 175$, 245, respectively, e.g., closer inspection of $|u|$ in Fig. 3 shows two possible subregions, before and after $n \sim 200$.

(iii) The shock speed of the hyperbolic system is

$$s = \frac{2r_+}{\sqrt{r_+ + r_-}}, \tag{3.4}$$

where r_+, r_- are the values of $|u|$ behind, and ahead of the jump, respectively.[14] We here obtain these values numerically, e.g., in Fig. 3, we clearly have $r_- = 0.5$, and we also use $r_+ = 0.75$ (arguing as above). The resulting estimate for the speed from (3.4) is $s = 1.34$. Using the numerical (approximate) positions of the jump at different times, we calculate a constant speed of 1.2.

In the nonlocal problem, we see comparable effects. For $\delta > 0$ sufficiently small, and $\kappa \geq 0.5$, dam-break initial conditions lead to profiles with negligible amplitude in the dark region. For smaller κ, we see some oscillations in the amplitude of the dark region sites. Jump initial conditions $u_1 = 1.0$, $u_2 = 0.5$ lead to some oscillations in both regions, especially near the interface, but no evidence of traveling wave structures transporting "density" $|u|$ to the darker region. This is indicated in Fig. 4, where the interface remains at its initial position $n = 261$.

For larger δ, we see dispersive shock phenomena, as in the local DNLS above. One of the main features seen for κ sufficiently small is a smoothing of some features

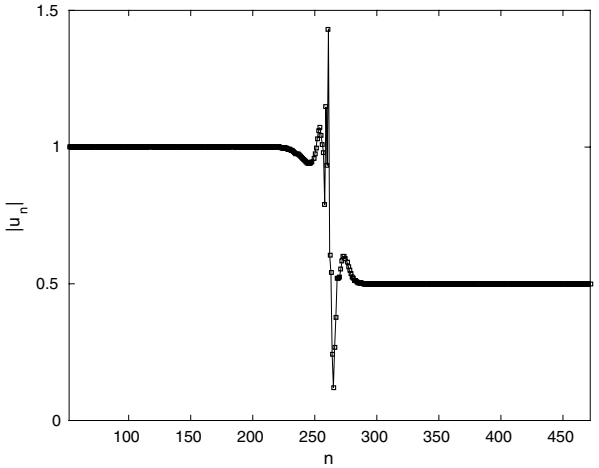

Fig. 4. Amplitude $|u_n|$ versus n at time $t = 60$, integration of (2.1). Initial condition $u_n = 1$ for $n \leq 261$, $u_n = 0.5$ for $n > 261$. $N = 523$, $\delta = 0.5$, $\gamma = -1.0$, $\kappa = 0.5$.

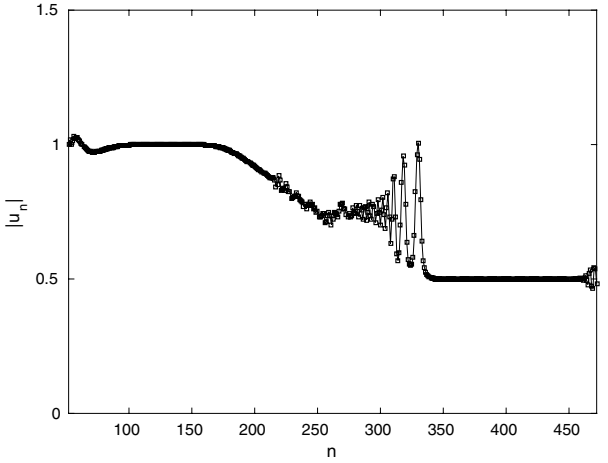

Fig. 5. Amplitude $|u_n|$ versus n at time $t = 60$, integration of (2.1). Initial condition $u_n = 1$ for $n \leq 261$, $u_n = 0.5$ for $n > 261$. $N = 523$, $\delta = 0.5$, $\gamma = -1.0$, $\kappa = 0.5$.

of the profile, e.g., the leading jump, as well as the apparent slope discontinuity at the leftmost point of the rarefaction wave. These features are indicated in Fig. 5, where $\kappa = 0.5$, and the other parameters are as in Fig. 3. For instance, the rough, i.e., 1–2 site period oscillatory region behind the jump seen in Fig. 3 now has the appearance of a train of solitary waves. The leading wave has a width of about 12 sites. The speed of the leading jump is however almost identical to the one we see in the local DNLS, see Fig. 3. In other experiments with the same parameters, e.g., the initial conditions of Fig. 2, the leading jump moves faster as we decrease κ, but smoothing is only evident in structures that are further behind the leading jump.

In the focusing case, dam-break initial conditions lead to some interesting dynamics, with large amplitude fluctuations in the bright region and a slow transfer of energy to the dark region. In Fig. 6, we see the onset of the amplitude fluctuations in the bright region, where we see amplitudes in the range of $[0.1, 1.8]$. We also see fluctuations at the numerical boundary. As time progresses, the amplitude fluctuations fill the entire left half of the domain, while the amplitude at the dark region remains relatively small. For instance, integrating the initial condition of Fig. 6 to a longer time $t = 90$, we have $|u_n| \leq 0.3$ for $n \in [262, 350]$, and $|u_n| \leq 0.05$ for $n > 350$. The above observations concern the parameter range $\kappa \geq 2.5$, where nonlocality seems to have a minor effect, seen mostly in the dark region. The slow increase of the amplitude in the dark region may be slightly enhanced by unstable modes with some appreciable amplitude in the dark region, see Ref. 11 for some indirect evidence of such modes in the finite shelf problem.

The results presented in this section are preliminary. A more detailed study for the local DNLS in Ref. 15 considers small amplitude jumps in the long wave limit, e.g., comparisons with numerics use a jump of size smaller that 10^{-1}. The discrete

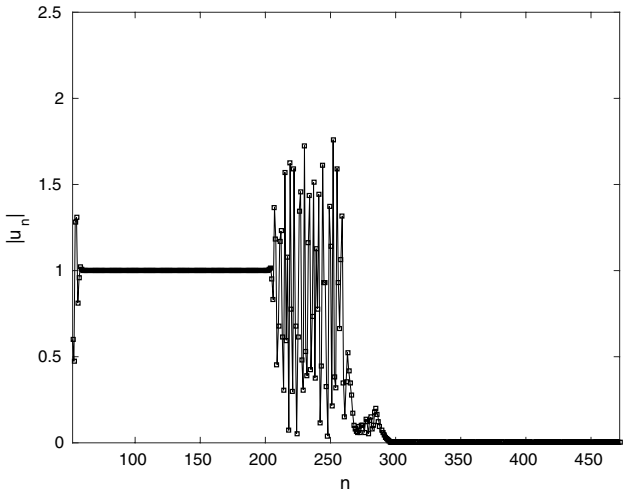

Fig. 6. Amplitude $|u_n|$ versus n at time $t = 30$, integration of (2.1). Initial condition $u_n = 1$ for $n \leq 261$, $u_n = 0.5$ for $n > 261$. $N = 523$, $\delta = -0.5$, $\gamma = -1.0$, $\kappa = 2.5$.

system is then approximated by KdV-type equations and dispersive shocks are analyzed in more detail. We have no analogous theory at present for the oscillations trailing the jump. KdV solutions may be relevant to the smoothed oscillations in Fig. 4.

4. Discussion

The present study was motivated in part by the idea that, in the defocusing discrete NLS equations and nonlocal analogues such as the Fratalocchi–Assanto model,[6] the local dynamics around breathers may be related to the onset of dispersive shock phenomena.

The present paper provides evidence that such an onset is indeed possible, and that it would be controlled by the linear intersite coupling δ. On the other hand, the validity and usefulness of the general idea requires more numerical work, and a more precise theoretical concept. It would be desirable for instance to study numerically the continuation of breather solutions from their $\delta = 0$ limit, examine possible changes in the local dynamics as δ is increased, and correlate such changes with the appearance of dispersive shock behavior. The above idea applies to dam-break initial conditions. Its extension to more general jump conditions would require a study of solutions with different limiting values at $\pm\infty$. This problem seems to be still open, but the presence of 2-torus generalizations of breathers may be possible by the theory of Ref. 18.

Our study raises other interesting problems. One is to understand the approximation of discrete dispersive shock phenomena by solutions of continuous models. Also of interest are the unstable shelf-solutions, and the related evolution of dam-break initial conditions of the focusing DNLS.

Acknowledgments

The author acknowledges partial support from Grants SEP-Conacyt 177246, Papit IN103916 and FENOMEC.

References

1. D. N. Christodoulides and R. I. Joseph, Discrete self-focusing in nonlinear arrays of coupled waveguides, *Opt. Lett.* **18** (1988) 794.
2. P. G. Kevrekidis, *The Discrete Nonlinear Schrödinger Equation* (Springer, New York, 2009).
3. M. Peccianti, G. De Luca, G. Assanto, C. Umeton and I. C. Khoo, Electrically assisted self-confinement and waveguiding in planar nematic liquid crystal cells, *Appl. Phys. Lett.* **77** (2000) 79.
4. C. Conti, M. Peccianti and G. Assanto, Route to nonlocality and observation of accessible solitons, *Phys. Rev. Lett.* **91** (2003) 073901.
5. M. Peccianti and G. Assanto, Nematicons, *Phys. Rep.* **516** (2012) 147–210.
6. A. Fratalocchi and G. Assanto, Discrete light localization in one-dimensional nonlinear lattices with arbitrary nonlocality, *Phys. Rev. E* **72** (2005) 066608.
7. A. Fratalocchi, G. Assanto, K. A. Brzdakiewicz and M. A. Karpierz, Discrete propagation and spatial solitons in nematic liquid crystals, *Opt. Let.* **29** (2004) 1530–1532.
8. A. Fratalocchi, G. Assanto, K. A. Brzdakiewicz and M. A. Karpierz, Discrete light propagation and self-trapping in liquid crystals, *Opt. Express* **13** (2005) 1808–1815.
9. K. A. Rutkowska, G. Assanto and M. A. Karpierz, Discrete light propagation in arrays of liquid crystalline waveguides, in *Nematicons*: *Spatial Optical Solitons in Nematic Liquid Crystals*, ed. G. Assanto (Wiley, Hoboken, 2013).
10. Y. K. Kartashov, V. A. Vysloukh and L. Torner, Soliton shape and mobility in optical lattices, *Prog. Opt.* **52** (2009) 63–148.
11. R. I. Ben, L. C. Ake, A. A. Minzoni and P. Panayotaros, Localized solutions for a nonlocal discrete NLS equation, *Phys. Lett. A* **379** (2015) 1705–1714.
12. R. I. Ben, J. P. Borgna and P. Panayotaros, Properties of some breather solutions of a nonlocal discrete NLS equation, Preprint (2016).
13. G. A. El, V. V. Geogjaev, A. V. Gurevich and A. L. Krylov, Decay of an initial discontinuity in the defocusing NLS hydrodynamics, *Physica D* **87** (1995) 186–192.
14. G. A. El and N. F. Smyth, Radiating dispersive shock waves in non-local optical media, *Proc. R. Soc. A* **472** (2016) 20150633.
15. A. M. Kamchatnov, A. Spire and V. V. Konotop, On dissipationless shock waves in a discrete nonlinear Shrödinger equation, *J. Phys. A* **37** (2004) 5547–5568.
16. R. S. MacKay and S. Aubry, Proof of existence of breathers for time-reversible or Hamiltonian networks of weakly coupled oscillators, *Nonlinearity* **7** (1994) 1623–1643.
17. D. E. Pelinovsky, P. G. Kevrekidis and D. J. Frantzeskakis, Stability of discrete solitons in nolinear Schrödinger lattices, *Physica. D* **212** (2005) 1–19.
18. D. Bambusi and D. Vella, Quasi periodic breathers in Hamiltonian lattices with symmetries, *Discrete Contin. Dyn. Syst. B* **2** (2002) 389–399.